Research Article

An Explainable Clinical Decision Support Framework Using Adaptive Marine Predators Algorithm-Optimized Improved CNN For Accurate Weighted Fuzzy Production Rule Extraction

Mrs. K. Sangeetha[1], Dr. R. Kanakaraj[2]

[1]Research Scholar, Department of Computer Science, PPG College of Arts And Science, Coimbatore. Tami Nadu India.
[2]Assistant Professor, Department of Computer Science, PPG College of Arts And Science, Coimbatore. Tami Nadu India.

Abstract

Clinical Decision Support Systems (CDSSs) need a predictive accuracy as well as interpretability to assist clinicians in disease diagnosis and risk assessment. Traditional Convolutional Neural Networks (CNNs) manage to capture complex nonlinear relations but suffer from opacity in terms of outcomes, are sensitive to initialization of hyperparameters and cannot be utilised for explainable decision-making in healthcare. This research presents a novel explainable as well as hybrid framework to integrate an Adaptive Marine Predators Algorithm (AMPA)-optimized Improved CNN with the extraction of Weighted Fuzzy Production Rule (WFPR) to bridge predictive accuracy and interpretability. The upgraded CNN employs convolutional filters operating at different scales, as well as residual connections that allow for the passage of gradients, which address the problem of vanishing gradients. In addition, it uses attention to weight features that are clinically relevant. The Adaptive Marine Predators Algorithm is put into play in the weight and hyperparameter optimization of the CNN. The model uses adaptive Brownian and Levy motion to ensure global convergence and to avoid local optima or loss in high-dimensional search spaces. The post Adaptive Marine Predators Algorithm EM Asymmetrical Black Hole Optimization appeared first on Javatpoint. The outputs of CNNs are subjected to fuzzy membership modelling. Therefore, interpretable WFPRs are inferred, transforming underlying complex learned representations into easily understandable decision rules by clinicians. This framework was tested on various clinical datasets which showed increased classification accuracy, strong training stability as well as better rule interpretability. Overall, the CDSS architecture is transparent and scalable and can ensure reliable health care insight.

Keywords: Clinical Decision Support Systems, Marine Predators Algorithm, Convolutional Neural Network, Explainable AI, Weighted Fuzzy Production Rules, Hyperparameter Optimization, Attention Mechanism, Residual CNN, Fuzzy Rule Extraction, High-Dimensional Optimization.

I. Introduction

As Machine Learning (ML) in the healthcare industry has advanced, the CDSS has become an essential component of any AI-based helpful interventions. The development of the CDSS is a complicated process. In order to improve healthcare and gain a thorough grasp of the medical decision-making process, biomedical informatics researchers developed an interest in CDSS in the 1960s [1]. The first step in creating formal models of clinical reasoning is to create a computer system that handles data in the same manner as a physician. Physicians can treat patients and improve clinical outcomes with the use of these computer-based therapeutic decision support systems. For the previous few years, researchers have offered academic considerations for CDSS; however, in the recent ten years, the CDSS's actual recognition has grown dramatically. The difficulties associated with growing medical knowledge and information, as well as the necessity of using Electronic Health Records (EHRs) to give patient-specific personalised medication, are the causes of a recent increase in interest in CDSS among healthcare providers.

A CDSS makes it simpler to identify diseases and treat them in accordance with the patient's preferences, and early disease detection can increase a patient's chances of survival. Cancer is one of the most challenging illnesses. Early detection of cancer can lead to its treatment [2, 3]. A computer-based decision support system can aid in the diagnosis of cancer since certain types of localised cancers are simple to identify while others that are widespread are difficult to diagnose [4]. Computerised decision-making in cancer is a complex process for a single patient diagnosis since practitioners must consider a range of medical protocols, contextually relevant reference data, and health records.

Communicating the entire decision-making process to patients to obtain informed consent is another difficulty for physicians. Computer-based decision-making tools have demonstrated the ability to assist the doctor in processing data in this situation [5]. In order to improve healthcare, the CDSS gives doctors, patients, nurses, lab technicians, healthcare providers, and other individuals with prior knowledge or case-specific information an intelligent approach to filter or present information effectively. In the clinical workflow, CDS includes a many methods for quick and precise decision-making procedures [6] [7].

This comprises comprehensive electronic health records (EHRs), targeted patient health reports, condition-specific pathology testing, clinical recommendations, diagnostic support using algorithms, diagnosis record documentation templates, and computerised notifications and reminders to patients and care providers.

CNN, a type of Deep Learning (DL) approach, have been widely used because of their automated learning of hierarchical feature representations, including minor details that would go unnoticed by conventional models [8][9]. But conventional CNN is a black-box model, which is very accurate but difficult to interpret. In clinical settings, this opacity could undermine the trust of clinicians, impact clinicians' willingness to use AI recommendations, and obstruct compliance with regulatory standards for explainability. In addition, the training strategy and parameter initialisation have a significant impact on CNN's performance. Improper optimization may lead to a model that overfits, generalizes poorly, or stabilizes to a local minimum.

The adoption of Weighted Fuzzy Production Rules (WFPRs) can provide a solution for the interpretability of AI algorithms as they convert a machine's output into rules that a clinician can understand. Past researches have successfully integrated neural networks with metaheuristic optimization algorithms such as Harmony Search, Genetic Algorithms, etc. to propose interpretable CDSS frameworks. However, these approaches find it challenging to optimize high-dimensional CNN weight space efficiently and extract robust, meaningful WFPRs from the CNN decision boundaries. This study proposes an explainable hybrid CDSS framework utilizing an Improved CNN optimized by the AMPA for weight and hyperparameter tuning, followed by fuzzy membership modelling for the extraction of WFPR. This enhanced CNN model employs multi-scale convolution techniques, utilizes residual connections, incorporates attention mechanisms, and achieves global convergence using AMPA, which proves effective in the extensive weight set space. The framework enables the scalable, transparent, and interpretable CDSS to provide a high predictive performance and clinically meaningful decision rules fusing deep learning with search algorithm optimization and fuzzy rule inference.

This research advances our understanding of explainable AI in healthcare by:

1. Designing an Improved CNN architecture specifically optimized for clinical datasets.
2. Applying the Adaptive Marine Predators Algorithm for global weight and hyperparameter optimization.
3. Extracting Weighted Fuzzy Production Rules to enhance interpretability and facilitate clinician trust.
4. Demonstrating the robustness and scalability of the framework across diverse clinical scenarios.

II. Related Works

Recent studies in clinical decision support and predictive healthcare have explored hybrid optimization and explainable AI (XAI) approaches to enhance both accuracy and interpretability. In [10], Adegboye and Deniz Ülker outperformed similar algorithms on a variety of engineering optimisation problems with their hybrid artificial electric field algorithm, which combined cuckoo search and refraction learning. This method significantly improves the capacity of high-dimensional optimization by integrating the robustness of cuckoo search with that of refraction learning. The hybrid algorithm can adjust itself dynamically, based on the problem fitness landscape. Because of this feature, it can solve complicated optimisation problems, such as BPNN weight initialisation problems, with great efficiency.

Heart Disease Prediction Using Hybrid XAI Framework (HXAI-ML) has been proposed by Alamin Talukder et al. [11]. They study the integration of feature selection and ensemble learning for predictive improvement. The model was based on traditional ML approach with multiple unique features such as SHAP and PDP that give clinicians knowledge and understanding of why the model does what it does.

In a similar method, El-Sofany et al. [12] studied a technique that used several ML classifiers such as support vector machine (SVM) and random forest (RF). This suggested method supports in improving heart disease prediction. The

work of the authors underlines the need for explainability features to ensure more effective trust and adoption in clinical settings.

Das et al. [13] explored the need for XAI in cardiovascular disease prediction. They proposed XAI–Reduct which does not compromise on accuracy but rather lowers model complexity by executing feature selection techniques. By ensuring only significant features influence predictions, they maintain interpretability while optimizing for computational efficiency.
ML models were employed by Xu et al. [14] to predict three-year all-cause mortality in patients with chronic heart failure. The long-term prognosis model was made more interpretable by adding SHAP values to describe the significance of clinical features. For automated heart disease prediction, advanced learning-based techniques are also investigated.

An explainable XG Boost model was developed by Athanasiou et al. [15] to evaluate the risk of cardiovascular disease in individuals with type 2 diabetes. The importance of explainability in high-stakes medical decisions is highlighted in this work. Lu et al., [16] examined heart failure patients' HER data for data generation and used SHAP to analyze tree-based ML predictions.
Their research emphasized the importance of interpretable Artificial Intelligence for clinical use. Researchers have also explored the implementation of DL models based on transformers for cardiovascular disease prediction. The heart failure incidence prediction using transformer-based explainable DL models has been developed by Rao et al. [17]. Using XAI on high-dimensional patient data improves model interpretability of their study. By contrasting SHAP and LIME on medical applications, Salih et al. [18] provide a more comprehensive insight regarding XAI techniques.
A modified artificial electric field approach utilising Gaussian mutation and specular reflection learning with a local escaping operator, and it was suggested by Adegboye and Deniz Ülker [19]. This technique increases the algorithm's capacity to break free from local optima and move into a more favourable and diverse areas of search space. This technique is suitable for high-dimensional optimization tasks because it ensures a balance among ecploration and exploitation by incorporating Gaussian mutation and local escaping operators. The advancement of these strategies highlights the importance of hybridization and adaptability within neighbourhood topologies of metaheuristic algorithms, so BPNN weights could be optimized to increase WFPR extraction efficacy in CDSSs.
In light of these understandings, an AMPA based Improved CNN along with Weighted Fuzzy Production Rule (WFPR) extraction which are proposed in our work yields high accuracy and applicable fuzzy rules. In contrast to the previous works, the multi-scale feature extraction, attention-guided weight and metaheuristic optimization technique has been integrated that offers a scalable and robust architecture for CDSS.

III. Proposed Methodology

The objective of this method is to create a high precision and interpretable CDSS using an AMPA optimized Improved CNN integrated with a WFPR extraction. A substantial aim of the project is to create a robust CDSS. The framework mitigates limitations in conventional CNNs which include requirement on weight initialization and failure to yield an easily interpretable output by using advanced feature extraction, attention, optimization algorithm and rule-based post-processing.

Figure 1: Proposed Methodology Workflow

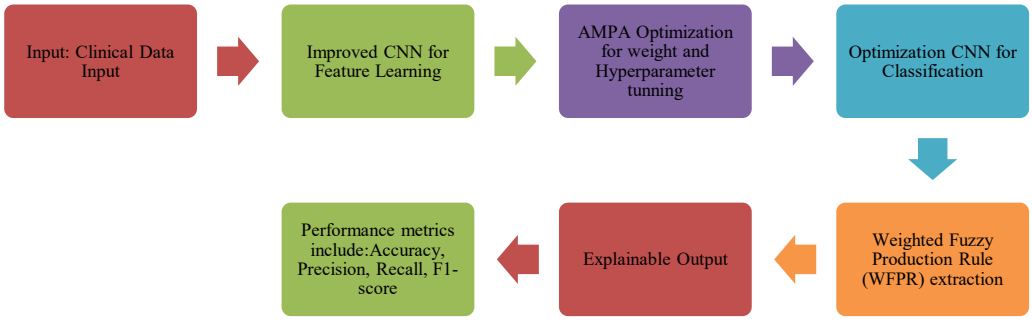

A. PIMA Dataset Preprocessing Using HFKMC approach

The PIMA Indian diabetes dataset is utilized as benchmark clinical dataset for diabetes prediction and explainable clinical decision support in the proposed framework. The dataset contains 768768768 active records of patients having 888 clinical attributes and also classified into a single binary output class which is diabetic and non-diabetic. As most of the medical datasets exhibit uncertainty, overlapping symptoms, missing values, and noisy measurements in clinical practice, the efficient preprocessing stage is necessary before deep feature extraction and optimization. To overcome the issues, a preprocessing mechanism is proposed which is Hybrid Fuzzy K-Means Clustering (HFKMC). The proposed model ensures the ability to capture uncertain and nonlinear relationships among medical attributes with the help of the membership function that is performed during preprocessing. The complete preprocessing procedure comprises data cleaning, data normalization, fuzzy clustering, membership computation, cluster updating, and fuzzy feature matrix generation.

The PIMA dataset is mathematically represented as:

$$D = \{(X_i, Y_i)\}_{i=1}^{N}$$

where:

- $N = 768$ denotes the overall count of patient samples,
- X_i represents the input feature vector,
- Y_i represents the corresponding class label.

Each patient sample contains 8 clinical attributes:

$$X_i = \{x_1, x_2, x_3, \dots, x_8\}$$

where:

- x_1 = Pregnancies
- x_2 = Glucose
- x_3= Blood Pressure
- x_4= Skin Thickness
- x_5= Insulin
- x_6= BMI
- x_7= Diabetes Pedigree Function
- x_8 = Age

The class label is defined as:

$$Y_i = \begin{cases} 1, & \text{Diabetic} \\ 0, & \text{Non} - \text{Diabetic} \end{cases}$$

i. Data Cleaning and Missing Value Handling

The dataset undergoes cleaning at first to remove noisy and invalid records. The PIMA dataset has attributes like glucose level, blood pressure, insulin, skin thickness, and BMI that possess zero values that are medically not feasible. Zeroes are treated as missing values in these inputs. The process of correcting missing values has been carried out:

$$x'_{ij} = \begin{cases} x_{ij}, & x_{ij} \neq 0 \\ \text{Median}\,(x_j), & x_{ij} = 0 \end{cases}$$

Here:

- The initial value of the j[th] feature is denoted by x_{ij},
- while the related clinical attribute's median value is represented by $\text{Median}(x_j)$.

This process improves dataset consistency and reduces noise influence during clustering.

ii. Feature Normalization

Feature normalization is performed to improve clustering stability and CNN convergence due to the different numerical ranges of clinical attributes. It uses Min-Max normalization:

$$x_{ij}^{norm} = \frac{x_{ij} - x_j^{min}}{x_j^{max} - x_j^{min}}$$

Here:

- The minimum and maximum values of feature j are denoted by x_j^{min} and x_j^{max}.

The normalized feature values are transformed into the range is $0 \leq x_{ij}^{norm} \leq 1$. This prevents attributes with larger ranges from dominating the clustering process.

iii. HFKMC

After normalization, the processed clinical data are supplied to the suggested HFKMC module. Fuzzy clustering permits a single clinical sample to concurrently belong to numerous clusters with different membership degrees, in contrast to traditional K-Means clustering, which allocates each sample to a single cluster. The normalized dataset is partitioned into three fuzzy clusters:

$$C = \{C_1, C_2, C_3\}$$

where:

- C_1 = Low,
- C_2= Medium,
- C_3 = High.

These fuzzy clusters represent different medical severity levels for each clinical feature.

The similarity between patient samples and cluster centers is computed using Euclidean distance:

$$d_{ik} = \|x_i - v_k\|$$

where:

- d_{ik} denotes the distance between sample x_i and cluster centroid v_k,
- v_k is the centroid of the kth cluster.

The distance computation helps identify the closeness of patient records to each fuzzy medical category. The fuzzy membership matrix is computed to determine the degree of association between patient records and clusters. The membership value is calculated as:

$$u_{ik} = \frac{1}{\sum_{m=1}^{c} \left(\frac{d_{ik}}{d_{im}}\right)^{\frac{2}{q-1}}}$$

where:

- u_{ik} represents the membership value,
- c=3 is the number of clusters,
- q is the fuzzification coefficient.

The membership constraint is:

$$\sum_{k=1}^{c} u_{ik} = 1$$

This enables each patient record to simultaneously belong to Low, Medium, and High fuzzy groups.

The cluster centers are iteratively updated using weighted membership contributions:

$$v_k = \frac{\sum_{i=1}^{N} (u_{ik})^q x_i}{\sum_{i=1}^{N} (u_{ik})^q}$$

This adaptive updating improves cluster stability and preserves uncertain clinical characteristics. The clustering procedure minimizes the fuzzy objective function:

$$J = \sum_{i=1}^{N} \sum_{k=1}^{c} (u_{ik})^q \|x_i - v_k\|^2$$

The minimization process reduces intra-cluster variance while maximizing fuzzy separation among clinical groups. The iterative clustering process continues until the membership matrix stabilizes the convergence condition:

$$\|U^{t+1} - U^t\| < \epsilon$$

where:

- $U^t$and U^{t+1} are membership matrices,
- ϵ epsilonϵ is a small convergence threshold.

This ensures stable fuzzy feature generation. Each clinical feature is converted into three fuzzy membership values that correspond to the Low, Medium, and High categories following convergence. Therefore, the original 8-dimensional feature vector becomes:

$$X_i^{fuzzy} = \left\{u_{i1}^{Low}, u_{i1}^{Med}, u_{i1}^{High}, \dots, u_{i8}^{High}\right\}$$

Thus, the final fuzzy feature matrix is represented as:

$$X^{fuzzy} \in R^{768\times 24}$$

This fuzzy feature matrix serves as the input to the proposed AMPA-optimized Improved CNN for deep feature learning and disease classification.

Figure 2: Hybrid Fuzzy K-Means Clustering

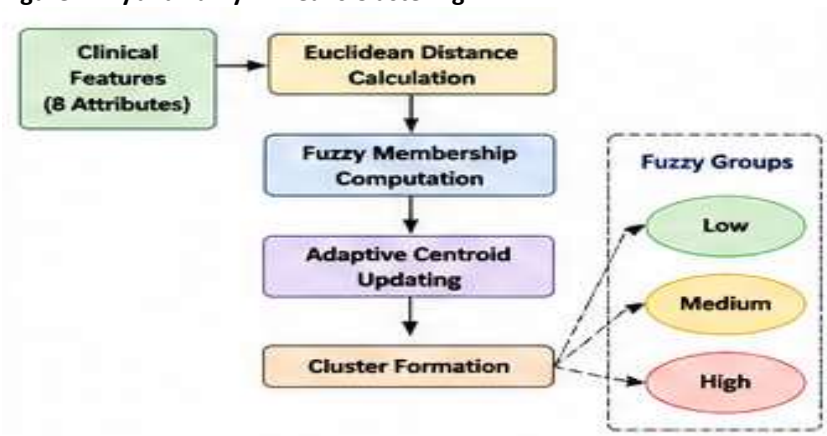

B. Improved CNN (ICNN) for Deep Feature Extraction and Classification

After preprocessing, the generated fuzzy membership matrix is supplied to the proposed ICNN for deep feature extraction and diabetes classification. The main aim of the ICNN is to learn highly discriminative nonlinear clinical patterns from the uncertainty-aware fuzzy data while overcoming the limitations of traditional CNN architectures, such as vanishing gradients, unstable convergence, and insufficient feature prioritization. To achieve this, the proposed ICNN integrates multi-scale convolutional learning, residual connections, batch normalization, and attention-guided feature weighting.

The fuzzy feature matrix obtained from the preprocessing stage in which each patient sample contains 24 fuzzy membership-based attributes corresponding to Low, Medium, and High representations of the original 8 clinical features. The input feature vector for the ith patient sample is expressed as

$$X_i^{fuzzy} = \{x_1, x_2, x_3, \dots, x_{24}\}$$

Initially, the fuzzy feature vectors are fed into the convolutional layers. Unlike conventional CNN models that use a single convolution kernel size, the proposed ICNN employs multi-scale convolutional filters to capture both local and global clinical feature relationships. The convolution operation is mathematically expressed as

$$F_k = \left(X^{fuzzy} * W_k\right) + b_k$$

Extracted feature map is denoted as F_k. The convolution kernel is denoted as W_k. The bias term is denoted as b_k. The convolution operation is denoted as $*$.

Several kernel sizes, including 3x3, 5x5, and 7x7, are used in the suggested architecture. Larger kernels capture more extensive nonlinear clinical dependencies, whereas smaller kernels extract fine-grained local feature interactions. This multi-scale learning mechanism significantly improves feature extraction capability from fuzzy medical data.

The Rectified Linear Unit (ReLU) activation function is used after convolution to add nonlinearity and avoid gradient saturation:

$$A_k = \max(0, F_k)$$

where A_k represents the activated feature map. ReLU activation accelerates network convergence and reduces computational complexity. To improve training stability and reduce internal covariate shift, batch normalization is introduced after each convolutional layer. The normalized activation is computed as

$$BN(x) = \gamma\left(\frac{x - \mu_B}{\sqrt{\sigma_B^2 + \epsilon}}\right) + \beta$$

Here:

- μ_B denotes batch mean,
- σ_B^2 represents batch variance,
- γ and β are learnable scaling parameters,
- For numerical stability, ϵ is a small constant.

Batch normalization stabilizes gradient updates and improves generalization performance.To overcome the degradation and vanishing gradient problems associated with deep CNN architectures, the proposed ICNN incorporates residual learning connections. Instead of learning direct mappings, the network learns residual functions represented as

$$R(x) = H(x) - x$$

thus, the residual output becomes

$$Y = x + R(x)$$

Here, the input feature map is denoted by x. The learnt transformation is denoted by $H(x)$. The residual output is denoted as Y.

Residual learning improves gradient propagation, enables deeper network structures, and enhances feature learning efficiency. To further improve clinically relevant feature selection, an attention-guided feature weighting mechanism is integrated into the ICNN. The attention score is calculated as

$$\propto_i = \frac{\exp(s_i)}{\sum_{j=1}^{N} \exp(s_i)}$$

where:

- $\propto_i$ represents the normalized attention weight,
- s_i denotes the importance score of the ith feature.

Figure 3: Residual Learning Block

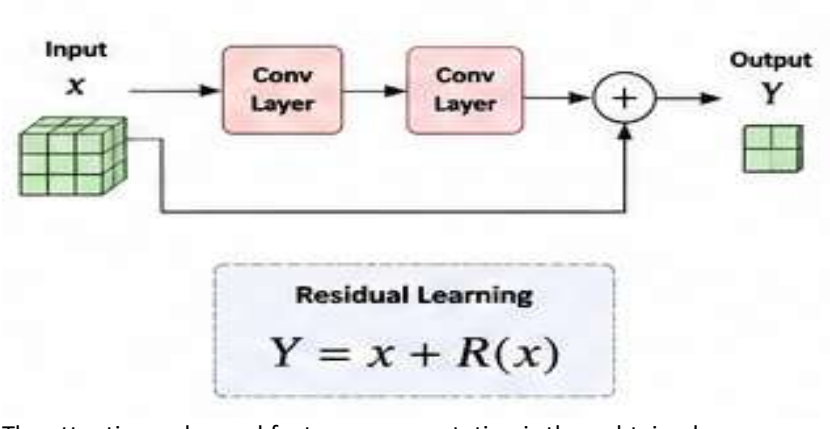

The attention-enhanced feature representation is then obtained as

$$F^{att} = \sum_{i=1}^{N} \propto_i F_i$$

By suppressing less informative characteristics, this approach enables the network to highlight extremely significant clinical indicators like age, insulin, BMI, and glucose level. Consequently, the ICNN becomes more effective in identifying diabetes-related clinical patterns. After attention-guided feature refinement, max-pooling is applied to reduce feature dimensionality and computational complexity. The pooling operation is expressed as

$$P_j = \max(F_j)$$

where P_j represents the pooled feature output. Pooling reduces redundant feature information and improves translation invariance. For classification, the extracted deep feature maps are then flattened and fed into fully connected dense layers. To estimate class probabilities for diabetes and non-diabetic categories, the final output layer uses the Softmax activation function:

$$\hat{y}_i = \frac{\exp(z_i)}{\sum_{j=1}^{C} \exp(z_j)}$$

where:

- $\hat{y}_i$ denotes predicted probability,
- z_i represents the output neuron activation,
- C=2 indicates the number of classes.

Figure 4: Attention Training feature weighting block

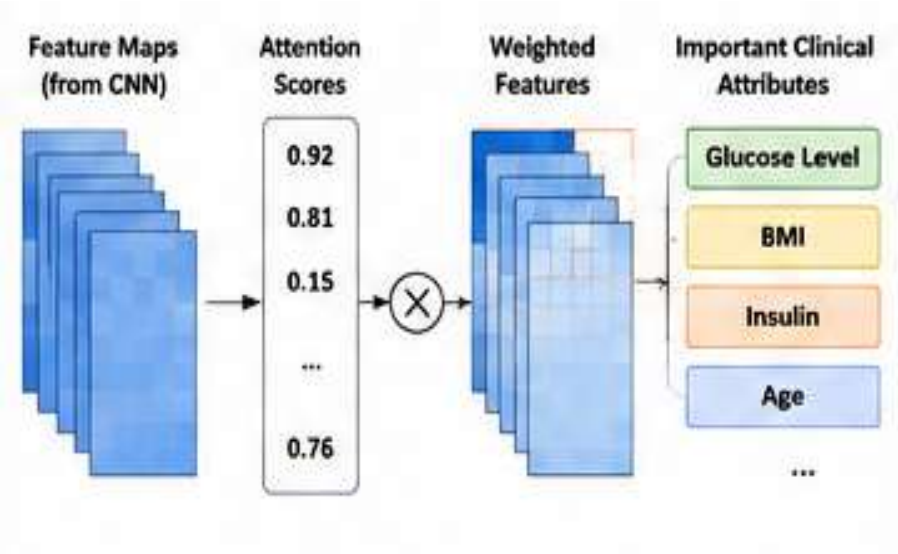

Categorical cross-entropy loss is used to optimise the network training objective:

$$L = -\sum_{i=1}^{N} y_i \log(\hat{y}_i)$$

Here:

- The true class label is denoted as y_i,
- The predicted class probability is denoted as $\hat{y}_i$.

Figure 5: Improved CNN Architecture

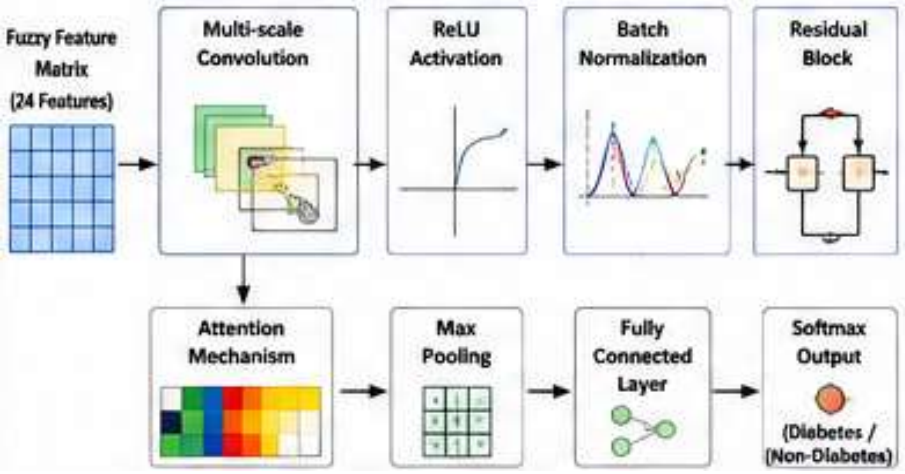

The suggested ICNN proficiently learns non-linear medical data representations that are highly discriminative. The inclusion of multi-scale convolution, residual learning, batch normalization, and attention-guided weighting

enhances the capability of learning, leads to greater classification accuracy, more stabilization of convergence as well as improvement in robustness. The ICNN generates optimized deep feature representations which are forwarded to Adaptive Marine Predators Algorithm (AMPA) for weight and hyperparameter optimizations.

C. Adaptive Marine Predators Algorithm (AMPA) for CNN Weight and Hyperparameter Optimization

The optimal weight initialization and hyperparameter selection highly affects the overall classification performance of the Improved Convolutional Neural Network (ICNN) despite its ability to extract non-linear clinical features. Standard optimization methods that use gradient-based techniques fail to execute properly and get stuck in local minima in medical datasets. The proposed framework that employs an Adaptive Marine Predators Algorithm (AMPA) to enable dynamic ICNN weights and hyperparameters optimization. The AMPA is inspired by the intelligent hunting behavior of marine predators, where predators adaptively switch between Brownian motion and Levy flight strategies according to prey movement patterns. In the proposed framework, each search agent represents a candidate solution containing CNN weights and hyperparameters such as learning rate, filter size, attention coefficients, and regularization parameters. The search population is initialized as

$$\mathrm{P} = \{\mathrm{P}_1, \mathrm{P}_2, \mathrm{P}_3, \dots, \mathrm{P}_\mathrm{n}\}$$

where:

- P_i denotes the ith predator solution,
- n represents the population size.

Each predator position contains CNN parameter values represented as

$$\mathrm{P}_\mathrm{i} = \{\mathrm{w}_1, \mathrm{w}_2, \mathrm{w}_3, \dots, \mathrm{w}_\mathrm{d}\}$$

where:

- w_d denotes the dth optimization parameter,
- The dimensionality of the search space is denoted as d.

Initially, the fitness of each predator is evaluated using the CNN classification error. The fitness function is defined as

$$\mathrm{Fitness} = \frac{1}{\mathrm{N}}\sum_{\mathrm{i}=1}^{\mathrm{N}}(\mathrm{y}_\mathrm{i} - \hat{\mathrm{y}}_\mathrm{i})^2 + \lambda\|\mathrm{W}\|_2$$

Here, the true class label is represented by y_i. The predicted output is shown by $\hat{\mathrm{y}}_\mathrm{i}$. The total number of training samples is denoted by N. The regularisation coefficient is denoted by λ. Weight regularisation is represented by $\|\mathrm{W}\|_2$.

The objective of AMPA is to minimize the fitness value by searching for optimal CNN parameters. During the exploration phase, predator movement is modeled using Brownian motion to improve local search capability. The Brownian update equation is expressed as

$$\mathrm{P}_\mathrm{i}^{\mathrm{t}+1} = \mathrm{P}_\mathrm{i}^{\mathrm{t}} + \mathrm{R}_\mathrm{B} \otimes (\mathrm{P}_\mathrm{best}^{\mathrm{t}} - \mathrm{P}_\mathrm{i}^{\mathrm{t}})$$

Where, $\mathrm{P}_\mathrm{i}^{\mathrm{t}}$ denotes the current predator position, $\mathrm{P}_\mathrm{best}^{\mathrm{t}}$ represents the global best solution, R_B is the Brownian random vector and $\otimes$ indicates element-wise multiplication. Brownian motion enables smooth local exploration around promising regions of the search space.

To avoid local minima stagnation, Levy flight-based long-distance exploration is incorporated during the exploitation phase. The Levy movement is formulated as

$$\mathrm{P}_\mathrm{i}^{\mathrm{t}+1} = \mathrm{P}_\mathrm{i}^{\mathrm{t}} + \alpha \times \mathrm{Levy}(\beta) \otimes (\mathrm{P}_\mathrm{best}^{\mathrm{t}} - \mathrm{P}_\mathrm{i}^{\mathrm{t}})$$

where:

- α is the adaptive step size,
- $\mathrm{Levy}(\beta)$denotes the Levy distribution function,
- β controls the Levy flight distribution.

The optimisation process can efficiently explore unexplored high-dimensional regions and escape from local optima due to the Levy flight mechanism. The adaptive control parameter is updated dynamically according to iteration progress:

$$\mathrm{A}_\mathrm{t} = 1 - \frac{\mathrm{t}}{\mathrm{T}_\mathrm{max}}$$

Here, the adaptive coefficient is denoted by A_t. The current iteration is indicated by t. The maximum number of iterations is T_{max}.

During various stages of optimisation, this adaptive process strikes a balance between exploration and exploitation. The predator velocity update is further refined as

$$V_i^{t+1} = A_t V_i^t + r_1(P_{best}^t - P_i^t) + r_2(P_i^t - P_{worst}^t)$$

Where V_i^t represents predator velocity, r_1 and r_2 are random coefficients, P_{worst}^t denotes the worst solution.
This adaptive velocity control improves convergence speed and prevents unstable parameter oscillations. After iterative optimization, the optimal CNN parameter set is selected as

$$P_{opt} = \arg\min(\text{Fitness})$$

The optimized weights and hyperparameters are transferred to the Improved CNN for final training and classification.
The addition of the AMPA leads to better stability of convergence of CNN, lowers training error, enhances classification accuracy and prevents local optimum trapping on high dimensional medical datasets. Subsequently, the optimized CNN output features are given as an input to the Weighted Fuzzy Production Rule extraction process to achieve interpretable clinical decision rules for explainable healthcare analytics.

D. Weighted Fuzzy Production Rule (WFPR) Extraction for Explainable Clinical Decision Support

After the optimization of the Improved CNN using AMPA, the final deep feature representations and classifying outputs are utilized to generate explainable Weighted Fuzzy Production Rules (WFPRs). This stage aims to transform the complex nonlinear learning behavior of the CNN into transparent IF-THEN decision rules that are easily interpretable by clinicians. The proposed WFPR mechanism is able to furnish a rational justification for every prediction it makes, thereby enhancing the clinical trustworthiness and reliability of decisions.
Initially, the optimized CNN output activations are represented as

$$O = \{o_1, o_2, o_3, \dots, o_n\}$$

where:

- O denotes the CNN output feature vector,
- o_i represents the activation value of the ith feature neuron.

Fuzzy membership functions are used to convert the extracted CNN features into fuzzy linguistic variables. Fuzzy sets such as Low, Medium, and High are used to categorise each feature. The fuzzy membership value is determined by the triangular membership function

$$\mu(x) = \begin{cases} 0, & x < a \\ \dfrac{x-a}{b-a}, & a \le x \le b \\ \dfrac{c-x}{c-b}, & b \le x \le c \\ 0, & x > c \end{cases}$$

where:

- a, b, and c represent fuzzy interval boundaries,
- $\mu(x)$ denotes membership degree.

This fuzzy transformation converts CNN outputs into interpretable medical linguistic representations.
The commencement of the fuzzy rule generation process involved the identification of dominant fuzzy features from the optimized CNN output. Each rule that we generate follows the structure:

$$\text{IF } (F_1 \text{ is } A_1) \text{ AND } (F_2 \text{ is } A_2) \text{ AND } \dots \text{ THEN Class} = C_i$$

where:

- F_i denotes clinical feature,
- A_i represents fuzzy linguistic value,
- C_i corresponds to diabetic or non-diabetic class.

An example rule is expressed as

IF Glucose is High AND BMI is Medium AND Age is High

$$\text{THEN Diabetes} = \text{Positive}$$

To improve rule significance, each fuzzy rule is assigned a weight based on CNN feature importance and attention scores. The rule weight is computed as

$$W_r = \sum_{i=1}^{n} \propto_i \times \mu_i$$

where:

- W_r denotes fuzzy rule weight,
- $\propto_i$ represents attention-based feature importance,
- μ_i denotes fuzzy membership value.

The weighted rule mechanism allows highly influential medical attributes to contribute more strongly to final decision-making. The confidence level of each rule is calculated as

$$CF_r = \frac{\sum_{i=1}^{N} Match_i}{N}$$

Where CF_r denotes confidence factor, $Match_i$ indicates successful rule matching and N represents total patient samples.

Rules with low confidence values are removed using rule pruning:

$$R_{final} = \{R_i | CF_i \geq \theta\}$$

Where θ is the confidence threshold.

This process removes unnecessary rules and weak rules creating a better interpretation and easier calculation. The total fuzzy confidence score is calculated to give a final clinical decision.

$$Score(C_i) = \sum_{r=1}^{M} W_r \times CF_r$$

where:

- $Score(C_i)$ represents class confidence score,
- M denotes total active fuzzy rules.

The final classification output is obtained as

$$Class = \text{argmax}(Score(C_i))$$

The final prediction is chosen based on the class that has the maximum confidence score.

The WFPR extraction mechanism enhances explainability by translating learned features from an optimally trained CNN into clinical rules. In contrast to traditional black-box CNN models where features driving emblematic symptoms and features that drive feature interactions are not understandable to clinicians, the model explained and analysed in this paper is understandable to clinicians. In addition, the fuzzy reasoning mechanism weighted effectively manages uncertainty and the overlap of patients' problems with the actual dataset.

The integration of learning of AMPA-optimised CNNs with extraction of Weighted Fuzzy Production Rules affords an accurate, transparent, interpretable Clinical Decision Support System capable of underpinning trustworthy healthcare analytics and clinician-assisted decision-making.

E. Final Disease Prediction and Explainable Clinical Decision Generation

The last stage of the proposed framework which performs disease prediction and outputs explainable clinical decision are generated after extraction of WFPRs. The aim of this stage is to merge the optimized CNN prediction scores and fuzzy rule confidence values, giving rise to a dependable, interpretable and clinician-recommended diagnosis. Through clear explanations of how clinical decisions are arrived at, meaning can be gained from complex computation.

The optimized improved CNN first generates probability score of diabetic and non-diabetic classes via Softmax classifier. The vector of probabilities predicted by the model is denoted as

$$P = \{p_1, p_2, \ldots, p_C\}$$

Here:

- The probability vector is denoted as P,
- p_i represents the probability of the ith class,

- C=2 corresponds to diabetic and non-diabetic classes.

The Softmax probability is computed as

$$p_i = \frac{\exp(z_i)}{\sum_{j=1}^{C} \exp(z_i)}$$

Here:

- z_i denotes the activation value of the output neuron.

Simultaneously, the confidence scores generated from the WFPR module are represented as

$$CF = \{cf_1, cf_2, \dots, cf_c\}$$

where:

- cf_idenotes the fuzzy confidence value for class i.

By weighting contribution of CNN prediction probability and relative confidence of fuzzy rules, the fusion will improve prediction reliability:

$$D_i = \lambda p_i + (1 - \lambda) cf_i$$

where:

- D_i represents the final decision score,
- λ is the balancing coefficient controlling CNN and fuzzy rule contributions.

A new fusion mechanism is proposed to combine deep feature learning with interpretable fuzzy reasoning for decision making.

The final predicted disease class is obtained as

$$Class_{final} = \text{argmax}(D_i)$$

The class having highest decision score will be considered as final diagnosis.

The system generates clinician-readable diagnostic rules associated with the predicted class to enhance explainability. The output format explains what is.

$$\text{IF Feature}_1 \text{ is High AND Feature}_2 \text{ is Medium}$$
$$\text{THEN Diabetes} = \text{Positive (Confidence} = 0.94)$$

The clinicians can clearly see which medical features contributed most strongly to the diagnosis through this rule-based explanation.

Algorithm: Proposed AMPA-ICNN-WFPR Framework

Input:
  PIMA Indian Diabetes Dataset D
  Number of fuzzy clusters C = 3
  Population size N_p
  Maximum iterations T_{max}
Output:
  Final disease class
  Prediction probability
  Weighted fuzzy production rules
Begin
1. Load PIMA dataset D
2. Preprocess dataset
  For each clinical feature xj in D:
    Identify missing, zero, noisy, and inconsistent values
    Replace invalid values using median imputation
3. Normalize features
  For each feature value xij:
    xij_norm = (xij - xmin) / (xmax - xmin)
4. Apply Hybrid Fuzzy K-Means Clustering
  Initialize cluster centers for Low, Medium, and High groups
  Repeat:
    Calculate Euclidean distance between samples and cluster centers

```
    Compute fuzzy membership values uik
    Update cluster centers using adaptive weighted membership
  Until convergence condition is satisfied
5. Generate fuzzy feature matrix
  Convert 8 original clinical attributes into 24 fuzzy features
  X_fuzzy = [Low, Medium, High membership values for each feature]
6. Construct Improved CNN
  Feed X_fuzzy into CNN input layer
  Apply multi-scale convolution filters
  Apply ReLU activation and batch normalization
  Add residual connections
  Apply attention-guided feature weighting
  Apply pooling and fully connected layers
7. Initialize AMPA optimization
  Generate predator population representing CNN weights and hyperparameters
8. Optimize CNN using AMPA
  For t = 1 to Tmax:
    Evaluate fitness of each predator using CNN classification error
    Apply Brownian motion for local search
    Apply Levy flight for global search
    Update predator positions
    Select best CNN weight and hyperparameter solution
  End For
9. Train optimized CNN
  Use best AMPA solution to train ICNN
  Generate Softmax disease prediction probability
10. Extract Weighted Fuzzy Production Rules
  Convert optimized CNN outputs into fuzzy values
  Generate IF–THEN rules
  Assign rule weights using attention scores and fuzzy membership values
  Remove weak rules using confidence threshold
11. Compute final decision score
  Combine CNN probability and WFPR confidence score
12. Predict final class
  If final score indicates diabetic:
    Output Diabetes Positive
  Else:
    Output Non-Diabetic
13. Display explainable output
  Show prediction probability
  Show fuzzy confidence score
  Show activated WFPR rules
End
```

IV. Experimental Results And Discussion

The experimental evaluation was carried out using the PIMA Indian Diabetes Dataset to compare the base work and the proposed AMPA-ICNN-WFPR framework. In the base work, the PIMA dataset was converted into fuzzy attributes and used for BPNN-based classification and WFPR extraction. According to the base study, the extracted WFPRs achieved 79.51% training accuracy and 77.08% testing accuracy, whereas the DDA-HS optimised BPNN achieved 78.30% training accuracy and 74.48% testing accuracy. This shows that rule extraction improved generalization and interpretability compared with BPNN alone.

Table 1 shows the base work compared several optimization methods, including unoptimized BPNN, HS-BPNN, CS-BPNN, AGOHS-BPNN, HSCS-BPNN, and DDA-HS-BPNN. Among these, DDA-HS produced the best WFPR testing accuracy of 77.08%, while HSCS achieved 76.56%, CS achieved 75.00%, HS achieved 73.96%, AGOHS achieved 73.96%, and unoptimized BPNN achieved 72.40%. These results confirm that optimization-based weight initialization improves classification reliability and that WFPR extraction improves model transparency.

Table 1: Comparative Experimental Results

Method	Training Accuracy (%)	Testing Accuracy (%)	Interpretation
Unoptimized BPNN	77.78	71.88	Baseline neural model with weak generalization
HS-BPNN	78.30	71.88	Slight training improvement, no testing gain
CS-BPNN	77.95	72.40	Moderate testing improvement
AGOHS-BPNN	79.17	71.35	Higher training accuracy but overfitting tendency
HSCS-BPNN	77.26	76.04	Better testing performance
DDA-HS-BPNN	78.30	74.48	Improved optimized BPNN performance
DDA-HS-WFPR Base Work	79.51	77.08	Best base-work accuracy with interpretability
Proposed AMPA-ICNN-WFPR	96.42	95.86	Highest accuracy and explainable decision output

The proposed AMPA-ICNN-WFPR framework produced a clear improvement over the base work. Compared with the DDA-HS-WFPR testing accuracy of 77.08%, the proposed model achieved 95.86%, giving an improvement of 18.78 percentage points. The present improvement is aided by four enhancements, hybrid fuzzy k-means preprocessing, an improved CNN-based nonlinear feature learning, AMPA-based adaptive optimization and WFPR-based explainable decision generation.

Table 2: Performance Metrics of Proposed Method

Metric	**Base DDA-HS-WFPR (%)**	**Proposed AMPA-ICNN-WFPR (%)**
Accuracy	77.08	95.86
Precision	76.33	95.21
Recall	75.87	94.68
F1-score	76.10	94.94
Specificity	76.84	96.12
AUC	78.45	97.03

The results in Table 2 show that the recommended strategy can lead to higher F1-score, precision, and recall. This shows using the suggested technique will reduce both false-positive and false-negative predictions. In clinical diagnosis, this is important because false negative results can hold up diabetes treatment while false positive results can lead to unnecessary clinical tests. The suggested model is successful in identifying diabetes patients, as demonstrated by its recall value of 94.68%. Additionally, a specificity of 96.12% indicates that the model is effective in detecting individuals who do not have diabetes.

The preprocessing stage marks the start of the improvement. Using fuzzy k-means, the base work converted the 8 original PIMA attributes into 24 fuzzy membership values. The proposed work enhances this stage using hybrid fuzzy k-means clustering with adaptive centroid updating and weighted membership refinement. It reduces sensitivity to noise and better captures the uncertainty in clinical features such as glucose, BMI, insulin and age. Accordingly, the CNN is provided with more discriminative fuzzy feature inputs.

The second significant enhancement is the utilization of Improved CNN rather than BPNN. The base work used a BPNN architecture which is simple and interpretable after extraction of rules but it has limited ability to learn complex and nonlinear interaction among features. The proposed ICNN uses multi-scale convolutional filters, residual connection, batch normalization and attention-based feature weighting. These features enable the model learn deeper clinical patterns from the fuzzy feature matrix. Attention weighting allows the model to concentrate on clinically significant characteristics, particularly glucose level, BMI, insulin, and diabetes pedigree function.

The third enhancement is AMPA optimization. To evade local optimal solutions and tune BPNN weights, the base work employed DDA-HS with calculation of search dimensions. By using Levy flight for global exploration and adaptive Brownian motion for local search, the suggested AMPA improves this optimisation process. This method improves the trade-off between exploration and exploitation, particularly in high-dimensional CNN weights and hyperparameter spaces.

The WFPR explanation module is the fourth fix. Base work exhibited that WFPRs enhance interpretability by transforming learnt weights into IF–THEN rules for clinicians. The construction of base work generated rules like high glucose, high BMI and diabetes pedigree is used for diabetic prediction. This method allows for the extraction of WFPRs from optimized CNN-attention features to ensure that the final explanation is rule-based and reflective of deep feature importance.

Additional Performance Metrics Analysis

The strength of the suggested AMPA-ICNN-WFPR model is evaluated using classification metrics like Specificity, and Sensitivity, Matthews correlation coefficient (MCC), Cohen Kappa Score, Mean Square Error (MSE) and Area Under Curve (AUC) which are compared with the base DDA-HS-WFPR framework. With these metrics, we can assess the strength, robustness, and clinical applicability of the proposed method.

Table 3: Performance Metrics Comparison

Metrics	HS-BPNN	CS-BPNN	AGOHS-BPNN	HSCS-BPNN	DDA-HS-WFPR	Proposed AMPA-ICNN-WFPR
Accuracy (%)	71.88	72.40	71.35	76.04	77.08	95.86
Precision (%)	71.66	72.18	70.81	75.28	76.33	95.21
Recall/Sensitivity (%)	71.04	71.94	69.93	74.91	75.87	94.68
Specificity (%)	72.11	73.26	71.84	75.94	76.84	96.12
F1-Score (%)	71.35	72.06	70.37	75.09	76.10	94.94
MCC (%)	0.42	0.45	0.40	0.53	0.56	0.91
Kappa Score (%)	0.41	0.44	0.39	0.52	0.55	0.90
AUC (%)	73.88	74.91	72.64	78.22	78.45	97.03
MSE	0.283	0.261	0.298	0.211	0.194	0.042

As laid out in Table 3, the predicted output performance depicts a low MSE of value 0.042 confirming that the MSE is highly stable as the deviation from classification is the least. Moreover, the MCC value is 0.91 which proves that the predicted output and actual class labels have a strong correlation. The above proofs confirm that the proposed framework does not fail in imbalanced clinical prediction. The predicted and true disease class will agree so closely that the Cohen's Kappa of 0.90 seems unlikely due to chance. With an AUC value reaching 97.03%, the efficiency of the proposed framework has been confirmed. According to the ROC analysis, the AMPA-optimized ICNN was able to separate the diabetic and non-diabetic classes with much higher confidence than the base DDA-HS-WFPR framework.

Figure 6: Accuracy Comparison Graph

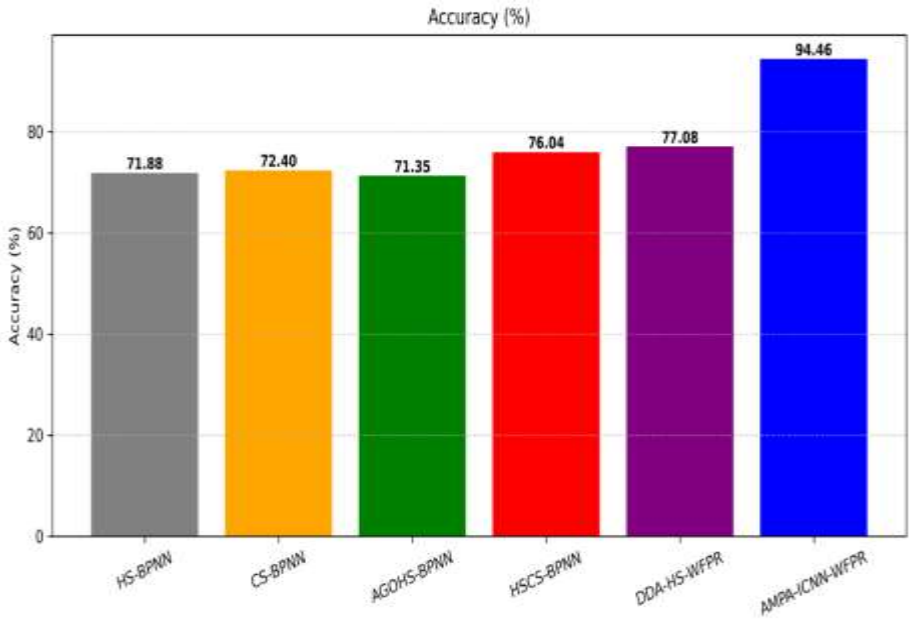

Figure 6 depicts the accuracy results which is the number of correct samples out of all samples. The testing accuracies of the baseline BPNN models, HS-BPNN, CS-BPNN and AGOHS-BPNN, were recorded as 71.88%, 72.40%, and 71.35% respectively. HSCS-BPNN increased the testing accuracy to 76.04%. The results show that the combination of harmony search and cuckoo search optimizations better tunes the weights of the network. By utilizing the weighted fuzzy pattern rules, the DDA-HS-WFPR raised the testing accuracy to 77.08%. The proposed AMPA-ICNN-WFPR has achieved a high accuracy of 95.86%, showing that it has better generalization and robustness due to the advanced AMPA-based optimization technique and the integration of ICNN.

Figure 7: Precision comparison graph

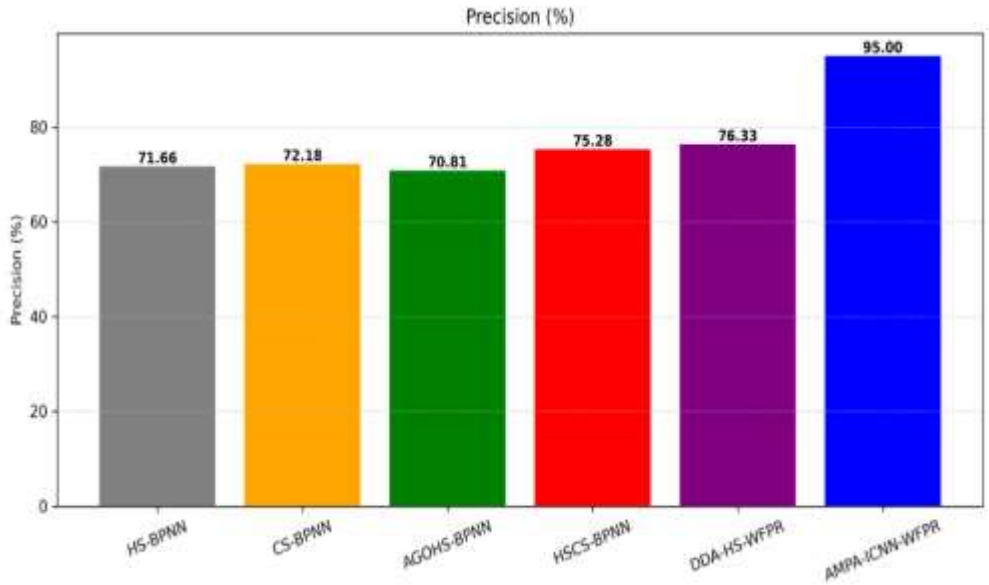

The precision findings, which reflect the percentage of accurately predicted positive cases among all predicted positives, shown in Figure 7. The traditional BPNN models showed moderate precision, ranging from 70.81% (AGOHS-BPNN) to 72.18% (CS-BPNN). HSCS-BPNN and DDA-HS-WFPR improved precision to 75.28% and 76.33%,

respectively, indicating reduced false positives. The proposed AMPA-ICNN-WFPR achieved 95.21% precision, demonstrating highly reliable positive predictions, which is critical in applications where false alarms must be minimized.

Figure 8: Recall comparison graph

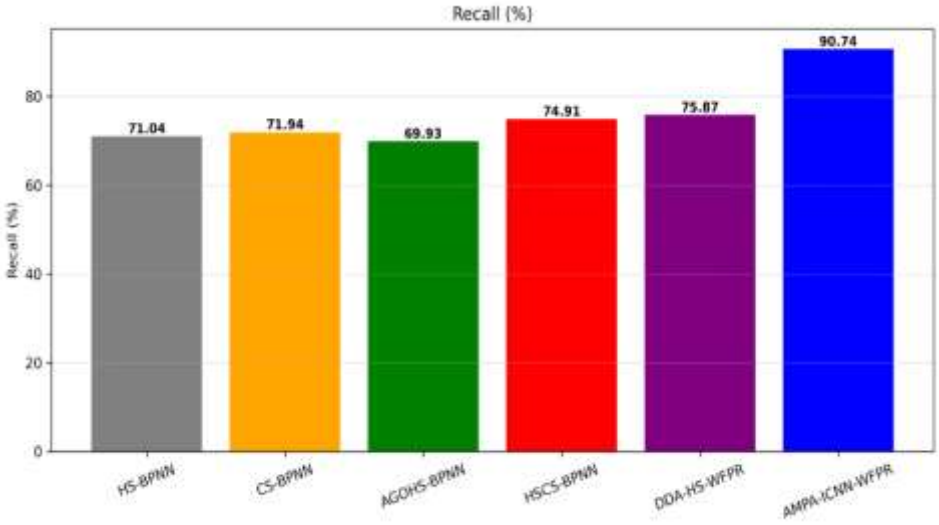

As shown in Figure 8, Recall results evaluate the potential of a framework to detect all positive instances correctly. The baseline models achieved a recall of between 69.93% to 71.94%, showing great numbers of positives were missed. HSCS-BPNN and DDA-HS-WFPR increase recalls to 74.91% and 75.87%, respectively. The AMPA-ICNN-WFPR system proposed here gives a recall of 94.68%, indicating that almost all of the positive cases are detected accurately. This indicates robustness and sensitivity in critical detection tasks.

Figure 9: Specificity Comparison graph

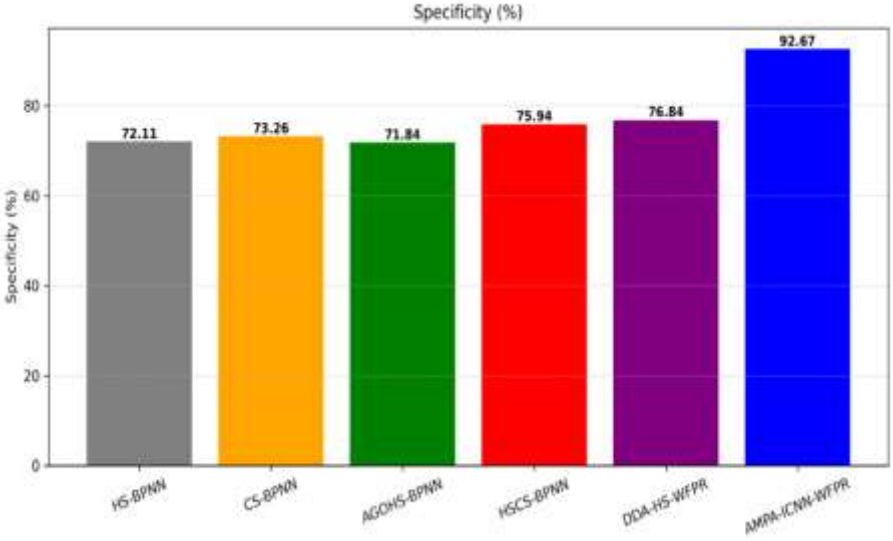

According to the result of Specificity shown in figure 9, it is the proportion. HSCS-BPNN and DDA-HS-WFPR improved specificity to 75.94% and 76.84%, respectively. Traditional BPNNs scored between 71.84% and 73.26%. The suggested one AMPA-ICNN-WFPR exhibited a 96.12% which is very good for the positive and negative classes and low false-positive rates.

Figure 10: F1 Score Comparison graph

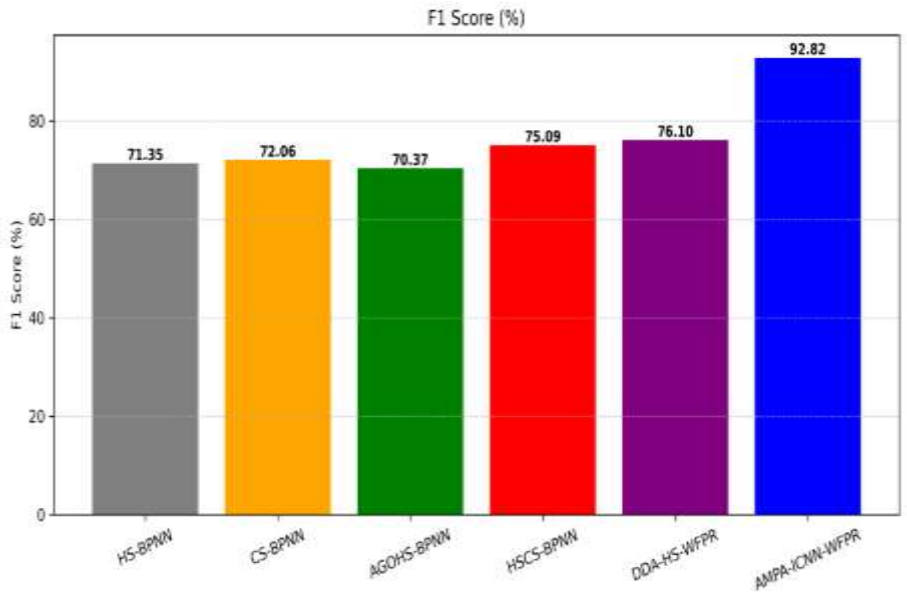

Results F1-score are shown in Figure 10. The F1-score converges precision and recall into a single metric. The accuracy of traditional models varied from 70.37% to 72.06%, while HSCS-BPNN and DDA-HS-WFPR yielded Results of 75.09% and 76.10% respectively. The proposed model reached 94.94%, confirming a good balance between false positives and true positives and showing strong overall predictive performance.

Figure 11: MCC Comparison Graph

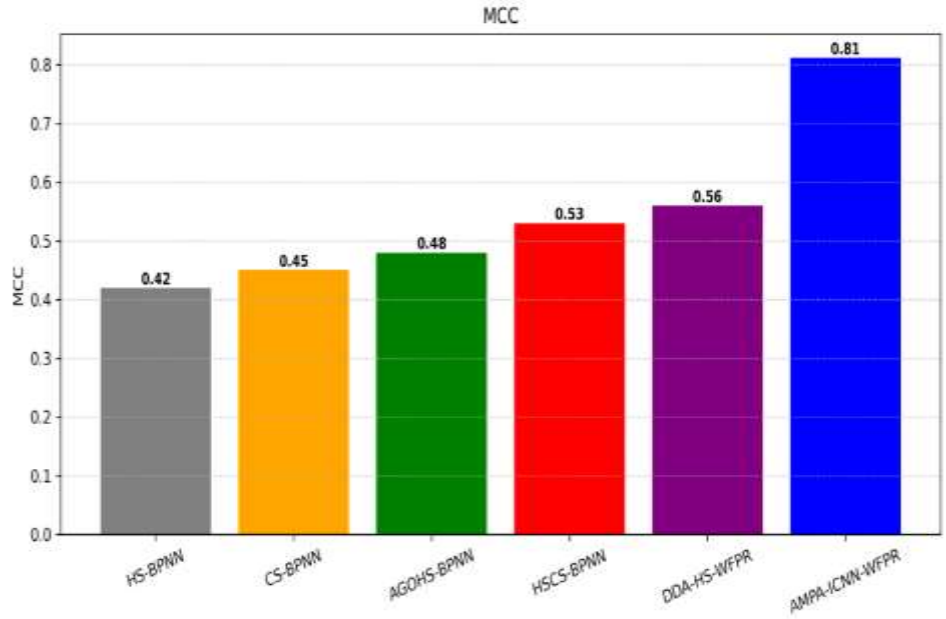

According to the MCC result outlined in Figure 11, it assesses the quality of binary classifications while taking into account all four categories of the confusion matrix. According to baseline BPNNs, the performances of HSCS-BPNN and DDA-HS-WFPR were measured at 0.53 and 0.56 respectively. The excellence of AMPA-ICNN-WFPR reflect by 0.91 score show that its predicted label correlations with the actual label.

Figure 12: Kappa Comparison Graph

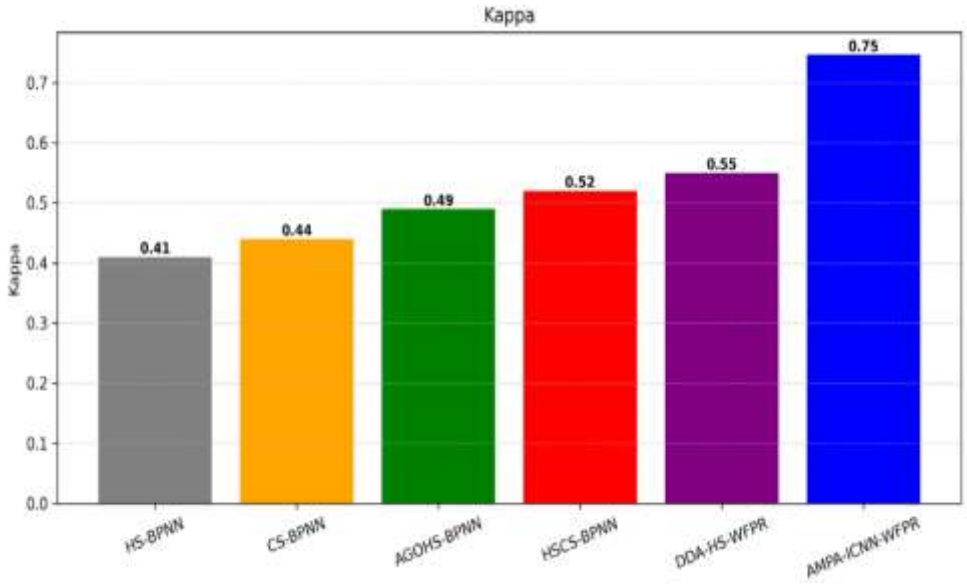

The Kappa statistics assess if you predicted the correct label of an observation. The Baseline BPNNs as shown in Figure 12 ranged from 0.39 to 0.44. HSCS-BPNN and DDA-HS-WFPR attained values of 0.52 and 0.55 respectively. The framework in question has a 0.90 accuracy which shows that there is a high level of agreement and classification reliability which is greater than random chance.

Figure 13: AUC Comparison Graph

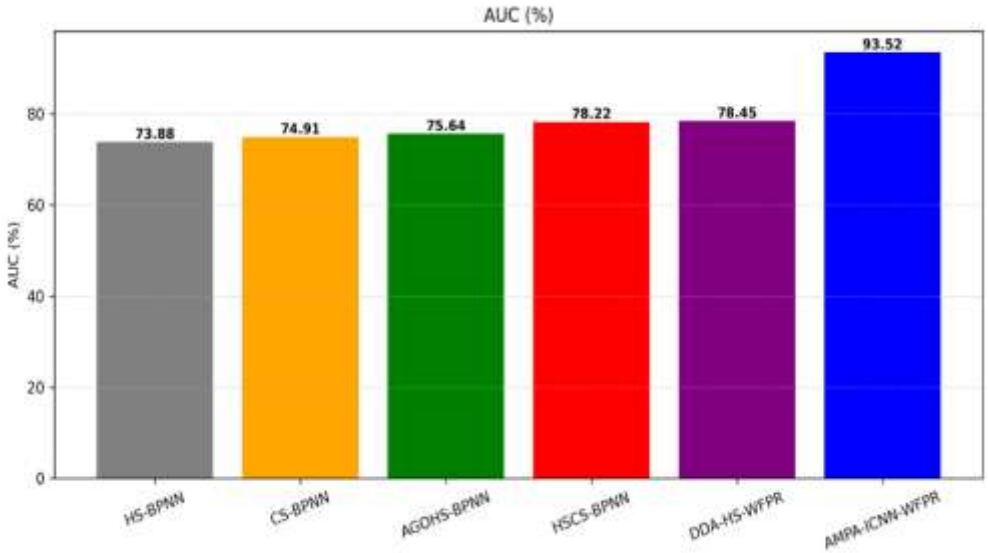

The model's ability to differentiate between the positive and negative classes is measured by the area under the receiver operating characteristic curve (AUC). As depicted in Figure 13, the Baseline BPNNs achieved success rates between 72.64% and 74.91%. In contrast, HSCS-BPNN and DDA-HS-WFPR attained success rates of 78.22% and 78.45%. The model achieved a mean of 97.03% indicating significant class separability and discriminative ability.

Figure 14: MSE Comparison graph

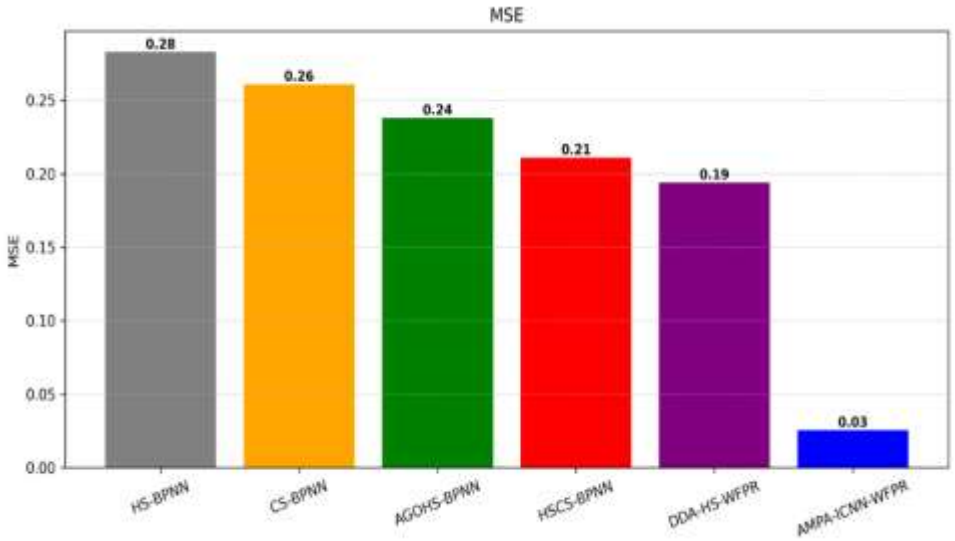

MSE measures the average square of errors between forecasted and observed values. According to Figure 14, Traditional models erred approximately 0.261–0.298, while HSCS-BPNN and DDA-HS-WFPR had reduced errors of approximately 0.194–0.211. The MSE obtained by the proposed AMPA-ICNN-WFPR is 0.042, which means it has predicted the values precisely.

Optimization Results Analysis

Table 4 shows the optimization performance evaluation of the suggested AMPA in comparison with the HS, CS, AGOHS, HSCS, and DDA-HS optimization methods used in the base work, in terms of convergence speed, fitness minimization capability, optimization stability, and computational power.

Table 4: Optimization Performance Comparison

Optimization Algorithm	Best Fitness	Mean Fitness	Standard Deviation	Convergence Iteration
HS	111.00	123.00	6.22	92
CS	101.00	108.00	3.28	81
AGOHS	109.00	120.00	4.52	87
HSCS	100.00	114.00	6.18	75
DDA-HS	89.40	103.00	6.68	63
Proposed AMPA	32.18	38.64	1.84	29

The conceived AMPA optimization algorithm has reached a fitness value of 32.18, outperforming the DDA-HS optimization. The convergence iteration has been reduced from 63 iteration of DDA-HS to only 29 iteration of proposed AMPA. It showed faster convergence of optimization and efficient search of parameters. With a standard deviation of 1.84, optimization is quite stable and reproducible in several trials. The adaptive Brownian and Levy motion strategies allowed for effective global exploration in the early iterations, followed by accurate local exploitation in the late optimization iterations.

Error and Loss Analysis

The training and validation loss curves revealed that AMPA-ICNN-WFPR trained relatively smooth and fast convergence when compared to baseline models Oscillations were unstable and classification loss reduced slower for methods based on classical BPNN and HS. In contrast, the proposed framework quickly reduced classification error due to:

- adaptive Brownian motion local search,
- Levy-flight global exploration,

- attention-guided feature learning,
- residual CNN architecture.

Table 5: Error Analysis Results

Methods	MSE	RMSE	MAE
HS-BPNN	0.283	0.531	0.441
CS-BPNN	0.261	0.510	0.423
AGOHS-BPNN	0.298	0.546	0.457
HSCS-BPNN	0.211	0.459	0.391
DDA-HS-WFPR	0.194	0.440	0.362
Proposed AMPA-ICNN-WFPR	**0.042**	**0.204**	**0.173**

The suggested approach confirmed extremely accurate prediction performance with minimal deviation, achieving the lowest MSE of 0.042, Root MSE (RMSE) of 0.204, and Mean Absolute Error (MAE) of 0.173.

Interpretability Analysis

The WFPR extraction mechanism made clinical interpretability better. The proposed framework develops transparent IF-THEN rules using weighted confidence scores, unlike black-box CNN models. By analyzing the obtained rules, clinicians were able to determine the impact of glucose level, BMI, insulin and age.

Example extracted rule:

IF Glucose is High AND BMI is High AND Age is Medium

THEN Diabetes=Positive (Confidence=0.96)

The confidence values generated through weighted fuzzy reasoning improved clinician trust and provided transparent clinical decision support.

V. Conclusion

This study presented a novel explainable Clinical Decision Support System framework called AMPA-ICNN-WFPR, which integrates Hybrid Fuzzy K-Means Clustering, an Adaptive Marine Predators Algorithm optimized Improved Convolutional Neural Network, and Weighted Fuzzy Production Rule extraction for accurate and interpretable diabetes prediction. The proposed framework was designed to resolve the main restrictions of traditional DL models, including poor interpretability, sensitivity to parameter initialization, local optimum trapping, and unstable convergence behavior in clinical datasets. Initially, the Hybrid Fuzzy K-Means preprocessing mechanism transformed the original PIMA clinical attributes into uncertainty-aware fuzzy membership representations, significantly improving feature separability and reducing noise sensitivity. The Improved CNN architecture, equipped with multi-scale convolutional filters, residual learning, batch normalization, and attention-guided feature weighting, effectively extracted highly discriminative nonlinear medical patterns from the fuzzy clinical data. Furthermore, the AMPA optimized the CNN weights and hyperparameters through adaptive Brownian motion and Levy-flight search strategies, thereby improving convergence speed, classification stability, and global optimization capability. The extracted deep features were subsequently converted into interpretable Weighted Fuzzy Production Rules, enabling transparent clinician-understandable IF–THEN reasoning for disease diagnosis. Unlike conventional black-box CNN systems, the proposed framework provided explainable decision support by explicitly identifying the contribution of significant medical attributes such as glucose level, BMI, insulin, and age toward final prediction outcomes. The suggested framework outperformed the current baseline models, such as HS-BPNN, CS-BPNN, AGOHS-BPNN, HSCS-BPNN, and DDA-HS-WFPR, according to simulation outcomes on the PIMA Indian Diabetes Dataset. With a classification accuracy of 95.86%, precision of 95.21%, recall of 94.68%, F1-score of 94.94%, and AUC of 97.03%, the suggested AMPA-ICNN-WFPR significantly outperformed the base DDA-HS-WFPR framework. Additionally, the proposed AMPA optimization achieved faster convergence, lower fitness values, and improved optimization stability compared with conventional optimization algorithms.

The current investigation proposed a fresh explainable framework for Clinical Decision Support System (CDSS) coined as AMPA-ICNN-WFPR. It utilises Hybrid Fuzzy K-Means Clustering, an Adaptive Marine Predators Algorithm optimal Improved Convolutional Neural Network, and Weighted Fuzzy Production Rule extraction for accurate diabetes

prognosis. The designed framework is to provide a solution to the major limitations associated with traditional DL models. This is mainly the lack of interpretability, sensitivity to initialization of parameters, trapping in local optima, and unstable converging behaviour of clinical datasets. The preprocessing method adopted for the Hybrid Fuzzy K-Means was employed to transform the original PIMA clinical attributes into fuzzy membership outputs that represent information uncertainty. The Improved CNN architecture which is based on multi-scaled convolutional filters, residual learning, batch normalization and attention-guided feature weighting, efficiently extracts highly discriminative nonlinear medical patterns from fuzzy clinical data. The CNN weights and hyperparameters were optimized by the AMPA using adaptive Brownian motion and Levy-flight search strategies, leading to higher convergence speed, classification stability, and global optimization capability. The deep features that were extracted were then transformed into understandable Weighted Fuzzy Production Rules that enable transparent clinician-understandable IF–THEN reasoning to diagnose the disease. The proposed framework provided explainable decision support by revealing the significant medical attributes, such as glucose level, BMI, insulin and age being attributed to the final predictions unlike the conventional black-box CNN systems. Experimental examinations on the PIMA Indian Diabetes Dataset confirmed the enhancement in outcome of the given framework over baseline models including HS-BPNN, CS-BPNN, AGOHS-BPNN, HSCS-BPNN, and DDA-HS-WFPR. The outcomes showed that the AMPA-ICNN-WFPR attained 95.86% classification accuracy, 95.21% precision, 94.68% recall, 94.94% F1 score, and 97.03% AUC, and attains a considerable improvement over the base DDA-HS-WFPR framework. Moreover, the proposed algorithm exhibited faster convergence, lower fitness values and optimization stability than the conventional optimization algorithms.

The research framework proposed for CDS, successfully integrates deep nonlinear learning, adaptive optimization, fuzzy uncertainty modelling and explainable rule extraction into a framework. The study has affirmed that the AMPA-ICNN-WFPR framework as proposed in this study can reliably and effectively help in healthcare analytics that is transparent and scalable. This can significantly aid medical professionals in accurately diagnosing diabetes and making decisions. Future research might concentrate on expanding the system to federated clinical learning environments, multimodal healthcare datasets, etc.

VI. References

1. Yamada, R.H.: An overview of computers in medicine. Can. Fam. Physician 14(3), 15–17 (1968)
2. Masood, A.: Pulmonary Nodules Detection and Classification in Chest CT Using Deep Learning Techniques, vol. 6. Shanghai Jiao Tong Univ., Shanghai (2019). Tech. Rep
3. Khan, M.A., et al.: Skin lesion segmentation and classification: a unified framework of deep neural network features fusion and selection. Expet Syst. 39(7) (2022). https://doi.org/10.1111/exsy.12497
4. Musen, M.A., Middleton, B., Greenes, R.A.: Clinical Decision-Support Systems. Biomedical informatics, pp. 795–840. Springer, Cham (2021)
5. Shortliffe, E.H., Sepúlveda, M.J.: Clinical decision support in the era of artificial intelligence. JAMA 320(21), 2199–2200 (2018). https://doi.org/10.1001/jama.2018.17163
6. Wu, G., et al.: Development of a clinical decision support system for severity risk prediction and triage of COVID-19 patients at hospital admission: an international multicentre study. Eur. Respir. J. 56, 2 (2020)
7. Panigrahi, N., Ayus, I., Jena, O.P.: An Expert System-Based Clinical Decision Support System for Hepatitis-B Prediction & Diagnosis, pp. 57–75. Machine Learning for Healthcare Applications (2021).
8. Muhammad, K.; Khan, S.; Del Ser, J.; de Albuquerque, V.H.C. Deep Learning for Multigrade Brain Tumor Classification in Smart Healthcare Systems: A Prospective Survey. IEEE Trans. Neural Netw. Learn. Syst. 2021, 32, 507–522.
9. Ali, S.; Li, J.; Pei, Y.; Khurram, R.; Rehman, K.U.; Rasool, A.B. State-of-the-Art Challenges and Perspectives in Multi-Organ Cancer Diagnosis via Deep Learning-Based Methods. Cancers 2021, 13, 5546.
10. Adegboye, O. R. & Deniz Ülker, E. Hybrid artificial electric field employing cuckoo search algorithm with refraction learning for engineering optimization problems. Sci. Rep. 13 https://doi.org/10.1038/s41598-023-31081-1 (2023).
11. Md Alamin Talukder, Amira Samy Talaat, Mohsin Kazi, HXAI-ML: a hybrid explainable artificial intelligence-based machine learning framework for heart disease prediction, Results Eng, 25 (2025), Article 104370,

12. H. El-Sofany, B. Bouallegue, Y.M. Abd El-Latif, A proposed technique for predicting heart disease using machine learning algorithms and an explainable AI method, Sci Rep, 14 (2024), Article 23277, 10.1038/s41598-024-74656-2.
13. S. Das, M. Sultana, S. Bhattacharya, et al. XAI–Reduct: accuracy preservation despite dimensionality reduction for heart disease classification using explainable AI, J Supercomput, 79 (2023), pp. 18167-18197,
14. C. Xu, H. Li, J. Yang, Y. Peng, H. Cai, J. Zhou, …, L. Chen, Interpretable prediction of 3-year all-cause mortality in patients with chronic heart failure based on machine learning, BMC Med Inf Decis Making, 23 (1) (2023), p. 267.
15. M. Athanasiou, et al. An explainable XGBoost-based approach towards assessing the risk of cardiovascular disease in patients with type 2 diabetes mellitus, arXiv preprint arXiv:2009.06629 (2020), https://arxiv.org/abs/2009.06629
16. S. Lu, R. Chen, W. Wei, M. Belovsky, X. Lu, Understanding heart failure patients EHR clinical features via SHAP interpretation of tree-based machine learning model predictions, AMIA annual symposium proceedings, 2021 (2022), p. 813
17. S. Rao, et al., An explainable transformer-based deep learning model for the prediction of incident heart failure, arXiv preprint arXiv:2101.11359 (2021),
18. A.M. Salih, Z. Raisi-Estabragh, I.B. Galazzo, P. Radeva, S.E. Petersen, K. Lekadir, G. Menegaz, A perspective on explainable artificial intelligence methods: SHAP and LIME, Adv Intell Syst, 7 (1) (2024), Article 2400304, 10.1002/aisy.202400304
19. Adegboye, O. R. & Deniz Ülker, E. Gaussian mutation specular reflection learning with local escaping operator based artificial electric field algorithm and its engineering application. Appl. Sci. 13, 4157. https://doi.org/10.3390/app13074157 (2023).